Hindawi
Complexity
Volume 2018, Article ID 4657235, 8 pages
https://doi.org/10.1155/2018/4657235

Research Article

Modeling and Dynamic Control of a Class of Semibiomimetic Robotic Fish

Shouxu Zhang[1], **Bo Jiang**[2], **Xiaoxuan Chen**[2], **Jian Liang**[3], **Peng Cui**[1], **and Xinxin Guo**[1]

[1]*School of Marine Science and Technology, Northwestern Polytechnical University, Xi'an 710072, China*
[2]*School of Information and Technology, Northwest University, Xi'an 710027, China*
[3]*State Key Laboratory of Transient Optics and Photonics, Chinese Academy of Sciences, Xi'an 710119, China*

Correspondence should be addressed to Shouxu Zhang; zhangshouxu@nwpu.edu.cn

Received 4 April 2018; Accepted 23 May 2018; Published 2 July 2018

Academic Editor: Andy Annamalai

This paper proposes a new robotic fish which avoids the complex mechanical structure and reduces the model complexity comparing to the existing bioinspired robotic fish, giving rise to a *semibiomimetic robotic fish*. The generalized Lagrange equation is adopted to establish the dynamic model of the robotic fish. The controllability of the system is analyzed, upon which a trajectory tracking control algorithm is designed by using the feedback linearization technique. The simulation results show that the dynamic model adopted in this paper can achieve better control performance.

1. Introduction

In 1960, Jack E. Steele first coined bionics [1], which applies biological methods or systems found in nature to design engineering systems. Over decades of development of modern bionics, the new interdisciplinary–biomimetic robotics (biorobotics) are proposed to design robots inspired from nature biological systems. In 1994, MIT developed the world's first free swimming robotic fish RoboTuna [2]. Since then, various types of robotic fish have been proposed [3, 4]. Hu et al. designed an autonomous robotic fish G9 that can swim in a 3D unstructured environment [5, 6]. Shen et al. designed a robotic dolphin with a pair of 3-DOF flippers and a multilink oscillatory propulsion mechanism to achieve the ability of lead-lag, feathering, and up-down motions [7]. Chen et al. designed a biomimetic robotic fish propelled by an ionic polymer-metal composite (IPMC) actuator to study general motions and maneuvers of the robotic fish [8]. Wang et al. designed a carangiform robotic fish and presented a new dynamic model for the system [9]. Low designed a robotic fish with modular undulating fins, owing to the special structure of the mechanical fin; the fish can swim with various modes [10].

Modeling and control of the robotic fish have been extensively studied in the following literature. Lighthill [11] first proposed a mathematical model of carangiform swimming fish based on slender-body theory. In [12], the large-amplitude elongated-body theory is proposed to analyze the hydrodynamics of carangiform swimming fish. Most of the existing robotic fish use large-amplitude elongated-body theory as mathematical model to analyze its motion control. Barrett et al. [13] developed a self-optimizing motion controller based on a genetic algorithm to achieve the optimal swimming motion for a robotic fish. A fuzzy logic and a PID control algorithm controller are used to achieve point-to-point swimming motion of a robotic fish [14]. Kelly et al. [15] use a digital approximation method to control the robotic fish swimming in 3 dimensions. An averaging dynamics method approach is proposed for the path planning and motion control for a kind of tail-actuated robotic fish [16]. Wang et al. and Zhao et al. [17, 18] use a central pattern 30 generator (CPG) to investigate the locomotion

control of a robotic fish, different from the large-amplitude elongated-body theory. Kopman et al. [19] use Kirchhoff's equations and Euler-Bernoulli beam theory to establish the dynamic model for a robotic fish; a PID control algorithm is used for the motion control of the system. In [20], the model of the robotic fish system is expressed in a control-affine transfer function; the state error feedback linearization is applied to realize the trajectory tracking control of the system. Barbera et al. and Yang et al. [21, 22] applied the extended Newton-Euler equation to present the dynamic model for a pectoral fin-driven robotic fish; a PID controller is used to achieve the attitude for the system. In [23], the Lagrangian function is used to establish the dynamic model of eel-like swimming robots; a perturbation analysis approach is applied to solve the control and motion planning for the system.

However, most of the above literature use fluid dynamics models based on the NS equation to fit fish's swimming numerically, and the motion control of robotic fish is limited to the motion control based on kinematics and variety of assumptions and models [24]. Therefore, there is no mature dynamic model for reference at present. To some extent, most results in the literature of robotic fish are still ad hoc in the sense that no rigorous results can be derived, either due to the difficulty of obtaining a rigorous dynamic model or due to the weak controllability of the system (mainly due to the too close mimicking of the natural fish). For instance, it is still unclear whether or not the mathematic dynamic model proposed therein can rigorously match the mechanical structure. The main reason may lie in the constraint of mimicking the natural fish motion in a too close (or too exact) manner; that is, the considered robotic fish in most existing results are trying to mimic the natural fish as adequately as possible, and in particular, the translation of the robotic fish is driven by the bending of the fish body.

In this paper, we propose a novel robotic fish system that installs a propeller at the end of the tail rather than bends their body or wavers the fins as in most existing results, inspired by the movie of showing the swimming of a robotic fish in [2, 25]; see Figure 1 for the basic mechanical structure of the proposed fish system. We refer to this robotic fish as *semibiomimetic robotic fish* since it only mimics a portion of characteristics of a natural fish (bending of the body shape is similar to a natural fish yet the driving force for translational motion is the thrust produced by the propeller at the tail end). The idea behind this choice is partly inspired from the aeroplane design (which can be considered to be a *semibiomimetic robotic bird*). It is well known that at the beginning period of aeroplane design, the aeroplane has been designed to maximally mimic the fly of real birds. However, such a design does not achieve the desired performance. In the later stage, with a large number of engineering practice and structural reform, the scientists ingeniously apply the fixed-wing plus jet engine to produce lift instead of fluttering wings. Such a *semibiomimetic design* (i.e., not too close to a natural bird) not only avoids the complex mechanical design but also reduces the model complexity. Similarly, by deriving the dynamic model of the proposed *semibiomimetic robotic fish system* here, we rigorously analyze the controllability of the system and it is shown that this kind of robotic system does have a good controllability, providing the potential applicability of the rigorous and fruitful nonlinear controllers. Specifically, we show that the feedback linearization approach can be used to ensure the exponential convergence of the closed-loop system as a time-varying desired trajectory is specified for tracking.

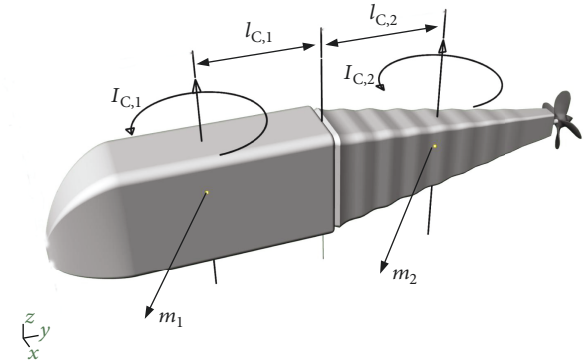

Figure 1: Mechanical structure of the proposed semibiomimetic robotic fish.

In summary, the main contribution of our work lies in two aspects: (1) the generalized Lagrangian approach is adopted to derive the dynamic equations of motion of a new class of robotic fish system (referred to as semibiomimetic robotic fish), yielding a rigorous dynamic model of the robotic fish, and (2) the controllability of the robotic fish system has been rigorously analyzed, and the feedback linearization algorithm has been proved to be able to cancel the nonlinear terms in the system and ensure the exponential stability of the closed-loop system. Our study and obtained results can thus be considered to be an ideal trade-off between the model-based controllability (concerning the dynamic model) and mechanical complexity (concerning the hardware aspect of the system).

The rest of the paper is organized as follows. Section 2 introduces the basic description of the robotic fish. In Section 3, we employ the Lagrange equation of the second kind (Euler-Lagrange) to get the dynamic equation of the system. The controllability of the system is examined in Section 4. Section 5 proposes a trajectory tracking control algorithm which uses the feedback linearization method to algebraically eliminate the severe nonlinearity of the system. Section 6 uses simulation results to verify the theoretical result. And some conclusions are summarized in Section 7.

2. Basic Description of the Robotic Fish System

The motion of the robotic fish is constrained to planar motion as shown in Figure 2. The robotic fish can be modeled as a system that consists of two rigid bodies (i.e., the body part and tail part) connected by a rotational

joint. The motion of the system can be described by specifying the translational and rotational motion of the body part and rotational motion of the tail part. The forces or torques that drive the motion of the system are the thrust $u \in R$ at the end point of the tail and the joint torque $\tau_m \in R$ exerted by the motor installed at the joint between the tail part and head part. Let (x_1, y_1) and (x_2, y_2) denote the position of the center of mass of the body and that of the tail, respectively. We use $X_I O_I Y_I$ and XOY to denote, respectively, the inertial coordinate frame and the body-fixed coordinate frame. Let $\theta \in R$ stand for the orientation between inertial coordinate frame and the body-fixed coordinate frame in counterclockwise, and $\alpha \in R$ represents the deflection angle with respect to the negative x-axis in counterclockwise.

The relation between the center of mass (CM) of the body part and tail part with respect to the inertial coordinate frame can be written as

$$\begin{bmatrix} x_2 \\ y_2 \end{bmatrix} = \begin{bmatrix} x_1 - l_{C,1}\cos\theta - l_{C,2}\cos(\theta+\alpha) \\ y_1 - l_{C,1}\sin\theta - l_{C,2}\sin(\theta+\alpha) \end{bmatrix}, \tag{1}$$

where $l_{C,1}$ and $l_{C,2}$ represent, respectively, the distance between the rotational joint and the CM of the robotic fish's body part and the distance between the rotational joint and the CM of the robotic fish's tail part.

3. Lagrangian Dynamics of Robotic Fish

We use the Lagrangian formulation to describe the dynamic behavior of the system [26–28]. The Lagrangian dynamics are derived by the following procedures.

Step 1. Choose the generalized coordinates.
We choose x, y, θ, and α to be the generalized coordinates to completely describe the state of the dynamic system.

Step 2. Write the Lagrangian of the system.
Since the gravity of the robotic fish is equal to its buoyancy, the total potential energy is zero. Therefore, the Lagrangian of the system can be written as

$$\begin{aligned} \mathscr{L} = {} & \frac{1}{2} I_{C,1}\dot{\theta}^2 + \frac{1}{2} I_{C,2}\left(\dot{\theta}+\dot{\alpha}\right)^2 \\ & + \frac{1}{2} m_1\left(\dot{x}_1^2 + \dot{y}_1^2\right) + \frac{1}{2} m_2\left(\dot{x}_2^2 + \dot{y}_2^2\right), \end{aligned} \tag{2}$$

where $I_{C,1}$ and $I_{C,2}$ denote, respectively, the inertia of the body part and that of the tail part. m_1 and m_2 denote, respectively, the mass of the body part and the mass of the tail part. Differentiating (1), one has

$$\begin{bmatrix} \dot{x}_2 \\ \dot{y}_2 \end{bmatrix} = \begin{bmatrix} \dot{x}_1 + l_{C,1}\sin\theta\dot{\theta} + l_{C,2}\sin(\theta+\alpha)\left(\dot{\theta}+\dot{\alpha}\right) \\ \dot{y}_1 - l_{C,1}\cos\theta\dot{\theta} - l_{C,2}\cos(\theta+\alpha)\left(\dot{\theta}+\dot{\alpha}\right) \end{bmatrix}. \tag{3}$$

Thus, (2) can be represented as the form

$$\begin{aligned} \mathscr{L} = {} & \frac{1}{2} I_{C,1}\dot{\theta}^2 + \frac{1}{2} I_{C,2}\left(\dot{\theta}+\dot{\alpha}\right)^2 + \frac{1}{2}(m_1+m_2)\left(\dot{x}_1^2+\dot{y}_1^2\right) \\ & + \frac{1}{2} m_2\left[l_{C,1}^2\dot{\theta}^2 + l_{C,2}^2\left(\dot{\theta}+\dot{\alpha}\right)^2 + 2l_{C,1}l_{C,2}\cos(\alpha)\left(\dot{\theta}^2+\dot{\theta}\dot{\alpha}\right)\right] \\ & + m_2\dot{x}_1\left[l_{C,1}\sin\theta\dot{\theta} + l_{C,2}\sin(\theta+\alpha)\left(\dot{\theta}+\dot{\alpha}\right)\right] \\ & - m_2\dot{y}_1\left[l_{C,1}\cos\theta\dot{\theta} + l_{C,2}\cos(\theta+\alpha)\left(\dot{\theta}+\dot{\alpha}\right)\right] \\ = {} & \frac{1}{2}\left[I_{C,1} + I_{C,2} + m_2 l_{C,1}^2 + m_2 l_{C,2}^2 + 2m_2 l_{C,1}l_{C,2}\cos(\alpha)\right]\dot{\theta}^2 \\ & + \left[I_{C,2} + m_2 l_{C,2}^2 + m_2 l_{C,1}l_{C,2}\cos(\alpha)\right]\dot{\theta}\dot{\alpha} \\ & + \frac{1}{2}\left[I_{C,2} + m_2 l_{C,2}^2\right]\dot{\alpha}^2 + \frac{1}{2}(m_1+m_2)\left(\dot{x}_1^2+\dot{y}_1^2\right) \\ & + m_2\dot{x}_1\left[\dot{\theta}(l_{C,1}\sin\theta + l_{C,2}\sin(\theta+\alpha)) + \dot{\alpha}l_{C,2}\sin(\theta+\alpha)\right] \\ & - m_2\dot{y}_1\left[\dot{\theta}(l_{C,1}\cos\theta + l_{C,2}\cos(\theta+\alpha)) + \dot{\alpha}l_{C,2}\cos(\theta+\alpha)\right]. \end{aligned} \tag{4}$$

Step 3. Write the equations of motion using the Lagrange equation of the second kind (Euler-Lagrange). The Euler-Lagrange dynamic equations of motion can be written as

$$\begin{aligned} f_1 &= a_1\ddot{x}_1 + [a_2\sin\theta + a_3\sin(\theta+\alpha)]\ddot{\theta} + a_3\sin(\theta+\alpha)\ddot{\alpha} + h_1, \\ f_2 &= a_1\ddot{y}_1 - [a_2\cos\theta + a_3\cos(\theta+\alpha)]\ddot{\theta} - a_3\cos(\theta+\alpha)\ddot{\alpha} + h_2, \\ \tau_1 &= [a_2\sin\theta + a_3\sin(\theta+\alpha)]\ddot{x}_1 - [a_2\cos\theta + a_3\cos(\theta+\alpha)] \\ &\quad \cdot \ddot{y}_1 + [a_4 + 2a_5\cos\alpha]\ddot{\theta} + [a_6 + a_5\cos\alpha]\ddot{\alpha} + h_3, \\ \tau_2 &= a_3\sin(\theta+\alpha)\ddot{x}_1 - a_3\cos(\theta+\alpha)\ddot{y}_1 + [a_6 + a_5\cos\alpha]\ddot{\theta} \\ &\quad + a_6\ddot{\alpha} + h_4, \end{aligned} \tag{5}$$

where f_1, f_2, τ_1, and τ_2 are the generalized forces acting on the system, and a_1, a_2, a_3, a_4, a_5, a_6, h_1, h_2, h_3, and h_4 are the equivalent parameters that can be chosen as

$$\begin{aligned} a_1 &= m_1 + m_2, \\ a_2 &= m_2 l_{C,1}, \\ a_3 &= m_2 l_{C,2}, \\ a_4 &= I_{C,1} + I_{C,2} + m_2 l_{C,2}^2 + m_2 l_{C,2}^2, \\ a_5 &= m_2 l_{C,1} l_{C,2}, \\ a_6 &= I_{C,2} + m_2 l_{C,2}^2, \\ h_1 &= a_2\cos(\theta)\dot{\theta}^2 + a_3\cos(\theta+\alpha)\left(\dot{\theta}^2 + \dot{\alpha}^2 + 2\dot{\theta}\dot{\alpha}\right), \\ h_2 &= a_2\sin(\theta)\dot{\theta}^2 + a_3\sin(\theta+\alpha)\left(\dot{\theta}^2 + \dot{\alpha}^2 + 2\dot{\theta}\dot{\alpha}\right), \\ h_3 &= -a_5\sin(\alpha)\dot{\alpha}\left(\dot{\alpha} + 2\dot{\theta}\right), \\ h_4 &= a_5\sin(\alpha)\dot{\theta}^2. \end{aligned} \tag{6}$$

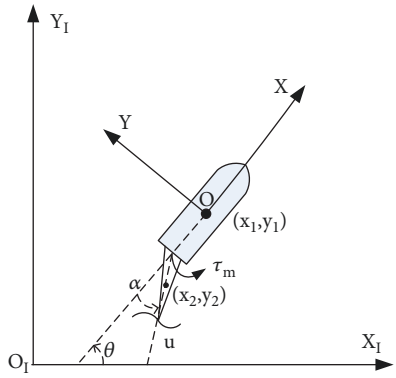

Figure 2: Robotic fish in a plane.

By incorporating the typical fluid drag forces into the dynamics (see, e.g., [29]), we have that

$$\begin{aligned}
&a_1\ddot{x}_1 + [a_2\sin\theta + a_3\sin(\theta+\alpha)]\ddot{\theta} + a_3\sin(\theta+\alpha)\ddot{\alpha} \\
&\quad + h_1 + c|\dot{q}|\dot{x}_1 = f_1, \\
&a_1\ddot{y}_1 - [a_2\cos\theta + a_3\cos(\theta+a)]\theta - a_3\cos(\theta+a)\ddot{a} \\
&\quad + h_2 + c|\dot{q}|\dot{y}_1 = f_2, \\
&[a_2\sin\theta + a_3\sin(\theta+\alpha)]\ddot{x}_1 - [a_2\cos\theta + a_3\cos(\theta+\alpha)]\ddot{y}_1 \\
&\quad + [a_4 + 2a_5\cos\alpha]\ddot{\theta} \\
&\quad + [a_6 + a_5\cos\alpha]\ddot{\alpha} + h_3 = \tau_1, \\
&a_3\sin(\theta+a)\ddot{x}_1 - a_3\cos(\theta+a)\ddot{y}_1 + [a_6 + a_5\cos\alpha]\ddot{\theta} \\
&\quad + a_6\ddot{\alpha} + h_4 = \tau_2,
\end{aligned} \tag{7}$$

where c is a positive constant, $q = [x_1, y_1]^T$, and $c|\dot{q}|\dot{x}_1$ and $c|\dot{q}|\dot{y}_1$ act as the fluid drag forces along the X and Y directions, respectively.

Note that it is assumed that the robotic fish in this work can be regarded as a two-rigid-body system that contains a revolute (rotational) joint. Due to these mechanical properties, the only two control inputs we can choose are the thrust u which is generated by the endpoint propeller and the exerted torque τ_m generated by the servo motor installed on the revolute (rotational) joint. We use Jacobian to represent the relationship among joint velocities, the endpoint velocities of the tail part, and the infinitesimal position relationship [30]. Indeed, the relationship can be obtained as follows:

$$\frac{d\mathbf{X}}{dt} = \mathcal{J}\frac{d\mathbf{Q}_i}{dt}, \tag{8}$$

where $\mathbf{X}$ is the endpoint position of the tail part. $\mathbf{Q}_i$ is the generalized coordinate. Thus, the Jacobian matrix J in this work can be written as

$$\mathcal{J} = \begin{bmatrix} 1 & 0 & l_{C,1}\sin\theta + l_{C,2}\sin(\theta+\alpha) & l_{C,2}\sin(\theta+\alpha) \\ 0 & 1 & -l_{C,1}\cos\theta - l_{C,2}\cos(\theta+\alpha) & -l_{C,2}\cos(\theta+\alpha) \end{bmatrix}. \tag{9}$$

Assume that there is no friction at the joint, then the external endpoint force F_{ext} and the joint exerted torque τ_{ext} can be converted to the equivalent generalized force τ, given by [26].

$$\tau = \tau_{\text{ext}} + J^T F_{\text{ext}}, \tag{10}$$

where $\mathcal{J}^T$ is the transpose of Jacobian. In this work, the external force is the endpoint thrust u, and the external torque is the exerted joint torque τ_m at the rotation joint of the robotic fish. Thus, (10) can be specifically expressed as

$$\begin{bmatrix} f_1 \\ f_2 \\ \tau_1 \\ \tau_2 \end{bmatrix} = \begin{bmatrix} 0 \\ 0 \\ 0 \\ \tau_m \end{bmatrix} + \mathcal{J}^T u R(\theta+\alpha)e_1, \tag{11}$$

where $R(\theta+\alpha)$ is a rotation matrix used to represent a rotation in the Euclidean space. Note that the coordinate of endpoint thrust in the body-fixed coordinate frame rotates counterclockwise through an angle $(\theta+\alpha)$ with respect to the origin of the inertial coordinate frame, and thus, the rotation matrix has the following form

$$R(\theta+\alpha) = \begin{bmatrix} \cos(\theta+\alpha) & -\sin(\theta+\alpha) \\ \sin(\theta+\alpha) & \cos(\theta+\alpha) \end{bmatrix}, \tag{12}$$

$e_1 = [1, 0]^T$, which means that the thrust u only has effects on the x-axis direction.

Finally, we can obtain the equivalent generalized force represented by the external force and torque

$$\begin{bmatrix} f_1 \\ f_2 \\ \tau_1 \\ \tau_2 \end{bmatrix} = \begin{bmatrix} \cos(\theta+\alpha)u \\ \sin(\theta+\alpha)u \\ l_{C,1}\sin(\alpha)u \\ \tau_m \end{bmatrix}. \tag{13}$$

Substituting the translational force $[f_1, f_2]^T$ in (13) into the first two equations in (7), we can obtain the translational dynamics

$$\begin{aligned}
a_1\ddot{x}_1 &= -[a_2\sin\theta + a_3\sin(\theta+\alpha)]\ddot{\theta} - h_1 - c|\dot{q}|\dot{x}_1 \\
&\quad - a_3\sin(\theta+\alpha)\ddot{\alpha} + \cos(\theta+\alpha)u, \\
a_1\ddot{y}_1 &= -[a_2\cos\theta + a_3\cos(\theta+\alpha)]\ddot{\theta} - h_2 - c|\dot{q}|\dot{y}_1 \\
&\quad + a_3\cos(\theta+\alpha)\ddot{\alpha} + \sin(\theta+\alpha)u.
\end{aligned} \tag{14}$$

Substituting the translational acceleration $[\ddot{x}_1, \ddot{y}_1]^T$ in (14) into the last two equations in (7), we can obtain the rotational dynamics

$$\begin{aligned}
(b_1 + 2b_2\cos\alpha)\ddot{\theta} + [b_3 + b_2\cos\alpha]\ddot{\alpha} + h_1^* &= \tau_1^*, \\
[b_3 + b_2\cos\alpha]\ddot{\theta} + b_3\ddot{\alpha} + h_2^* &= \tau_2^*,
\end{aligned} \tag{15}$$

with b_1, b_2, b_3, h_1^*, and h_2^* being of the form

$$\begin{aligned}
b_1 &= I_{C,1} + I_{C,2} + \frac{m_1 m_2}{m_1 + m_2}\left(l_{C,1}^2 + l_{C,2}^2\right),\\
b_2 &= \frac{m_1 m_2}{m_1 + m_2} l_{C,1} l_{C,2},\\
b_3 &= I_{C,2} + \frac{m_1 m_2}{m_1 + m_2} l_{C,2}^2,\\
h_1^* &= h_3 - \left[\frac{(h_1 + c|\dot{q}|\dot{x}_1)}{a_1}\right][a_2 \sin\theta + a_3 \sin(\theta+\alpha)]\\
&\quad + \left[\frac{(h_2 + c|\dot{q}|\dot{y}_1)}{a_1}\right][a_2 \cos\theta + a_3 \cos(\theta+\alpha)],\\
h_2^* &= h_4 - \left[\frac{(h_1 + c|\dot{q}|\dot{x}_1)}{a_1}\right][a_3 \sin(\theta+\alpha)]\\
&\quad + \left[\frac{(h_2 + c|\dot{q}|\dot{y}_1)}{a_1}\right][a_3 \cos(\theta+\alpha)],\\
\tau_1^* &= \tau_1 - \frac{m_2 l_{C,1}[\sin\theta f_1 - \cos\theta f_2]}{m_1 + m_2}\\
&\quad - \frac{m_2 l_{C,1}[m_2 l_{C,2}[\sin(\theta+\alpha) f_1 - \cos(\theta+\alpha) f_2]}{m_1 + m_2}\\
&= \tau_1 + \frac{-m_2 l_{C,1} \sin\alpha}{m_1 + m_2} u = -\frac{m_1 l_{C,1} \sin\alpha}{m_1 + m_2} u,\\
\tau_2^* &= \tau_m,
\end{aligned} \tag{16}$$

Thus, the final form of rotational dynamics can be rearranged as follows:

$$\begin{aligned}
(b_1 + 2b_2 \cos\alpha)\ddot{\theta} + (b_3 + b_2 \cos\alpha)\ddot{\alpha} + h_1^* &= -\frac{m_1 l_{C,1} \sin\alpha}{m_1 + m_2} u,\\
(b_3 + b_2 \cos\alpha)\ddot{\theta} + b_3\ddot{\alpha} + h_2^* &= \tau_m.
\end{aligned} \tag{17}$$

4. Controllability of the System

The translational dynamics (14) can be written in matrix form

$$a_1\ddot{q} = -c|\dot{q}|\dot{q} + \psi + \underbrace{\begin{bmatrix} -a_3 \sin(\theta+\alpha) & \cos(\theta+\alpha) \\ a_3 \cos(\theta+\alpha) & \sin(\theta+\alpha) \end{bmatrix}}_{B(\theta,\alpha)} \begin{bmatrix} \ddot{\alpha} \\ u \end{bmatrix}, \tag{18}$$

where

$$\psi = -\begin{bmatrix} [a_2 \sin\theta + a_3 \sin(\theta+\alpha)]\ddot{\theta} + h_1 \\ -[a_2 \cos\theta + a_3 \cos(\theta+\alpha)]\ddot{\theta} + h_2 \end{bmatrix}. \tag{19}$$

Consider the input transformation

$$v = -c|\dot{q}|\dot{q} + \psi + B(\theta,\alpha)[\ddot{\alpha}, u]^T, \tag{20}$$

and we have that

$$a_1\ddot{q} = v, \tag{21}$$

with q as the output and v as the control input. According to the *standard linear system theory*, this system is obviously controllable in the whole space of R^2. On the other hand, the above input transformation is nonsingular for all possible states of the system since $B(\theta,\alpha)$ is always nonsingular. This leads us to obtain the conclusion that the system (18) with q as the output and $[\ddot{\alpha}, u]^T$ as the control input is controllable in R^2.

Substituting the first equation in (17) into the second one gives the direct relation between τ_m and $\ddot{\alpha}$

$$\overbrace{\left[b_3 - \frac{(b_3 + b_2 \cos\alpha)^2}{b_1 + 2b_2 \cos\alpha}\right]}^{w(\alpha)} \ddot{\alpha} + \phi = \tau_m, \tag{22}$$

with

$$\begin{aligned}
\phi &= \left[-\frac{b_3 + b_2 \cos\alpha}{b_1 + 2b_2 \cos\alpha} h_1^* + h_2^*\right]\\
&\quad - \frac{m_1 l_{C,1} \sin\alpha (b_3 + b_2 \cos\alpha)}{(m_1 + m_2)(b_1 + 2b_2 \cos\alpha)} u.
\end{aligned} \tag{23}$$

Since $w(\alpha)$ is uniformly positive, the relation between τ_m and $\ddot{\alpha}$ is nonsingular. This result in combination with the above one yields the conclusion that the combined system given by (18) and (22) with q as the output and $[\tau_m, u]^T$ as the input is controllable over R^2.

5. Trajectory Control

Based on the previous controllability analysis, we show that the translational dynamic (18) can be transformed into a simple linear doubleintegrator system through the input transformation.

Assume that our task is to steer the fish from an arbitrary initial position to a desired trajectory. In this work, we use feedback linearization [31] to cancel the nonlinear term in the translational dynamics (18). For some constant-speed trajectory q_d (i.e., $\ddot{q}_d = 0$), the control laws can be specified as

$$v = -K_P(q - q_d) - K_D(\dot{q} - \dot{q}_d). \tag{24}$$

In the more general case, the desired trajectory may have variable speed (i.e., $\ddot{q}_d \neq 0$), and the control law can be designed as

$$v = \ddot{q}_d - K_P(q - q_d) - K_D(\dot{q} - \dot{q}_d), \tag{25}$$

with K_P and K_D being positive design constants.

Denote by $e = q - q_d$ the tracking error, and we then have that

$$a_1\ddot{e} + K_D\dot{e} + K_P e = 0, \tag{26}$$

which leads to an exponentially stable error dynamics and implies the exponential convergence of the tracking errors according to the standard linear system theory.

Table 1: Physical parameters of the robotic fish.

Bodies	m_i (kg)	$I_{C,i}$ (kg•m^2)	$l_{C,i}$ (m)
Head part	1.8000	0.4320	0.9000
Tail part	0.8000	0.2160	0.9000

Substituting the control law calculated in the form of (24) or (25) into (20), we can obtain the thrust and the (reference or desired) acceleration for the robotic fish as

$$\begin{bmatrix} \ddot{a} \\ u \end{bmatrix} = B^{-1}_{(\theta,\alpha)}(\nu + c|\dot{q}|\dot{q} - \psi). \tag{27}$$

As (22) gives the direct relationship between τ_m and $\ddot{\alpha}$, we can then design the motor torque as

$$\tau_m = \omega(\alpha)\ddot{\alpha} + \phi(u), \tag{28}$$

with $\ddot{\alpha}$ and u being calculated by (27). We have to emphasize that the control input (i.e., u and τ_m) calculation does not involve the measurement of $\ddot{\alpha}$, but it does need the measurement of $\ddot{\theta}$ since ν defined by (24) or (25) involves ψ which depends explicitly on $\ddot{\theta}$ [see (19)].

6. Simulation Results

In the simulation, we choose the origin of the inertial frame (reference frame) as the initial position of the robotic fish. The control inputs of the robotic fish are the endpoint thrust $u(t)$ and the exerted joint torque $\tau_m(t)$. The physical parameters of the robotic fish are shown in Table 1 and Figure 1, and the parameter c (for describing the fluid drag forces) is set as $c = 2.0$. For a desired trajectory $q_d(t)$, the control laws are in the form of (25) and (28). Here, we need to obtain the joint acceleration $\ddot{\theta}$ in order to compensate the nonlinear term in (24) or (25), and the acceleration $\ddot{\theta}$ can be estimated from the joint velocity $\dot{\theta}$ by using a "low-pass filter" [32, 33] in the form of

$$\ddot{\theta} = \frac{\lambda}{s+\lambda}\dot{\theta}, \quad s = \frac{d}{dt}, \tag{29}$$

where λ denotes the cut-off frequency of the filter. The sampling period is set as 5 ms.

6.1. Line-Path Tracking. In the first case, we consider the tracking of a ramp trajectory (i.e., a line path)

$$q_d(t) = \begin{bmatrix} -1t \\ -6t \end{bmatrix}, \tag{30}$$

and the desired velocity can then be written as

$$\dot{q}_d(t) = \begin{bmatrix} -1 \\ -6 \end{bmatrix}. \tag{31}$$

The controller parameters are set as $K_P = 10$, $K_D = 15$, and $\lambda = 3000$. Simulation results are shown in Figures 3 and 4,

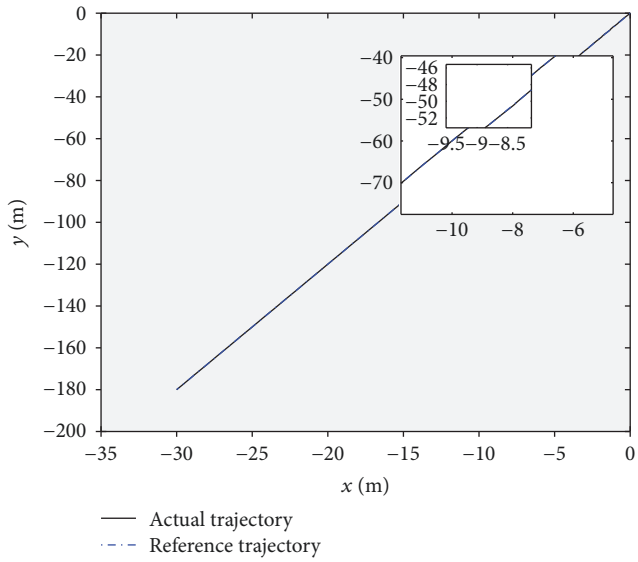

Figure 3: Position tracking (line-path tracking).

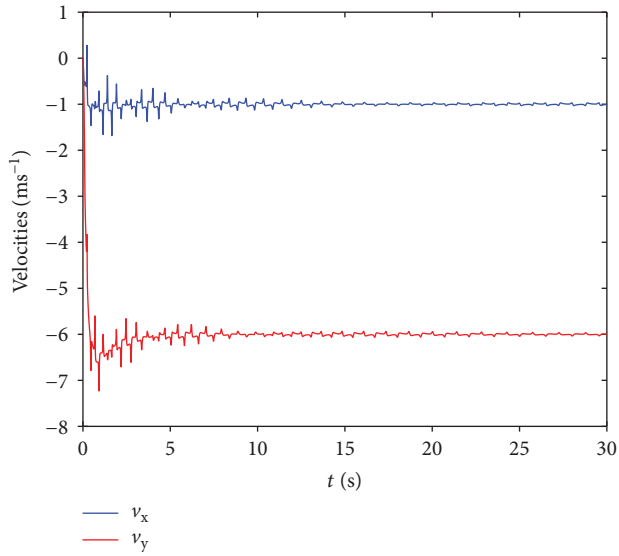

Figure 4: Velocity tracking (line-path tracking).

and we see that the position of the robotic fish asymptotically converges to the desired one.

6.2. Circle-Path Tracking. Consider now that the desired trajectory is a circle given by

$$q_d(t) = \begin{bmatrix} \cos(0.2\pi t) \\ \sin(0.2\pi t) \end{bmatrix}, \tag{32}$$

and the controller parameters are still the same as the case of line-path tracking. Simulation results are shown in Figures 5 and 6. Even in this case of complicated path, the convergence of the position tracking errors is still ensured.

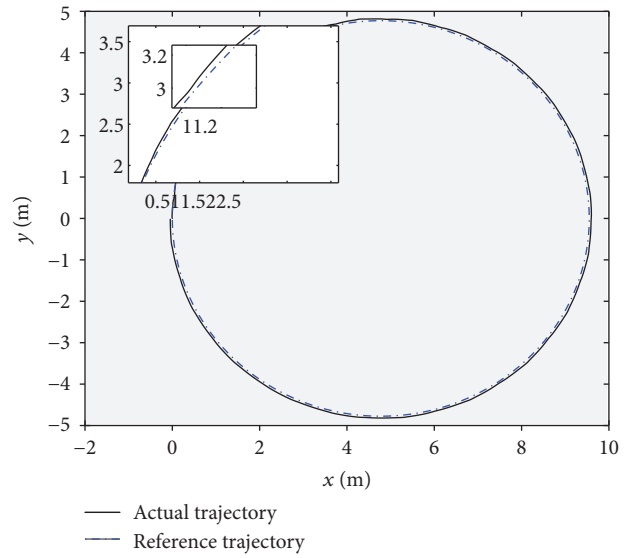

Figure 5: Position tracking (circle-path tracking).

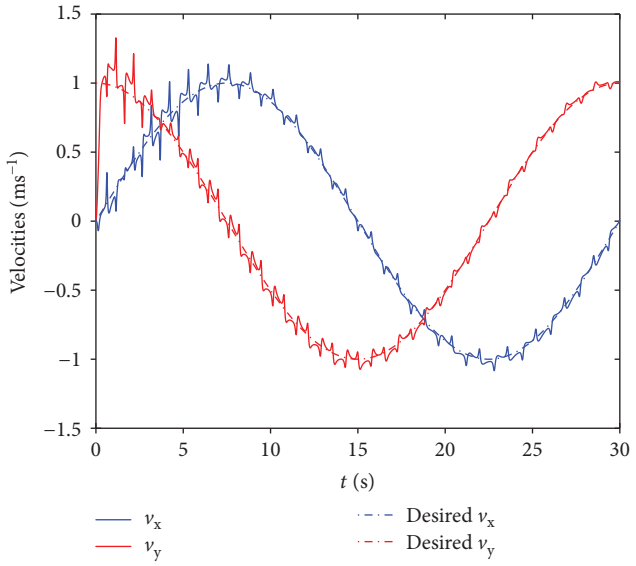

Figure 6: Velocity tracking (circle-path tracking).

7. Conclusions

In this paper, we proposed a novel robotic fish system which can be referred to as a semibiomimetic robotic fish (i.e., a tail-propulsion robotic fish) in contrast with most robotic fish in the literature. We derive its dynamics based on the Lagrange equation. Feedback linearization is employed to design the control inputs to avoid the severe nonlinearity in the system, and the convergence of the trajectory tracking errors is rigorously shown. Simulation results are provided to show the trajectory tracking performance of the system; in particular, the dynamic response of the proposed semibiomimetic robotic fish is acute, flexible, and fast, in contrast to most robotic fish systems in the literature (especially those that are (almost) completely biomimetic).

Future work includes the further investigation of the handling of the system model uncertainty, path planning and obstacle avoidance for robotic fish, and cooperative control of multiple robotic fish. The robotic fish system with multiple rotational joints would be another potentially important research direction since that would provide the system with more flexibility; for example, 3-dimensional motion can be achieved.

Data Availability

The data used to support the findings of this study are included within the article.

Conflicts of Interest

The authors declare that they have no conflicts of interest.

Acknowledgments

This work was supported by the National Natural Science Foundation of China under Grant nos. 61733014, 41601353, and 61633002; the Fundamental Research Funds for the Central Universities; the Natural Science Basic Research Plan in Shaanxi Province of China (no. 2017JQ4003); mitra2006-digital Scientific Research Project of Shaanxi Provincial Education Department (no. 17JK0766); and the Foundation of State Key Laboratory of Transient Optics and Photonics, Chinese Academy of Sciences (no. SKLST201614).

References

[1] M. H. Dickinson, "Bionics: biological insight into mechanical design," *Proceedings of the National Academy of Sciences*, vol. 96, no. 25, pp. 14208-14209, 1999.

[2] D. Barrett, "Mit ocean engineering testing tank biomimetics project: Robotuna," http://web.mit.edu/towtank/www/tuna/robotuna.html.

[3] G. Q. Sun, C. H. Wang, L. L. Chang, Y. P. Wu, L. Li, and Z. Jin, "Effects of feedback regulation on vegetation patterns in semi-arid environments," *Applied Mathematical Modelling*, vol. 61, pp. 200–215, 2018.

[4] H. Xiao, R. Cui, and D. Xu, "A sampling-based bayesian approach for cooperative multiagent online search with resource constraints," *IEEE Transactions on Cybernetics*, vol. 48, no. 6, pp. 1773–1785, 2018.

[5] H. Hu, J. Liu, I. Dukes, and G. Francis, "Design of 3d swim patterns for autonomous robotic fish," in *2006 IEEE/RSJ International Conference on Intelligent Robots and Systems*, pp. 2406–2411, Beijing, China, 2006.

[6] J. Liu, H. Hu, and D. Gu, "A hybrid control architecture for autonomous robotic fish," in *2006 IEEE/RSJ International Conference on Intelligent Robots and Systems*, pp. 312–317, Beijing, China, 2006.

[7] F. Shen, C. Wei, Z. Cao, D. Xu, J. Yu, and C. Zhou, "Implementation of a multi-link robotic dolphin with two 3-DOF flippers," *Journal of Computer Information Systems*, vol. 7, pp. 2601–2607, 2011.

[8] Z. Chen, S. Shatara, and X. Tan, "Modeling of biomimetic robotic fish propelled by an ionic polymer–metal composite

caudal fin," *IEEE/ASME Transactions on Mechatronics*, vol. 15, no. 3, pp. 448–459, 2010.

[9] J. Wang, F. Alequin-Ramos, and X. Tan, "Dynamic modeling of robotic fish and its experimental validation," in *2011 IEEE/RSJ International Conference on Intelligent Robots and Systems*, pp. 588–594, San Francisco, CA, USA, 2011.

[10] K. H. Low, "Locomotion and depth control of robotic fish with modular undulating fins," *International Journal of Automation and Computing*, vol. 3, no. 4, pp. 348–357, 2006.

[11] M. J. Lighthill, "Note on the swimming of slender fish," *Journal of Fluid Mechanics*, vol. 9, no. 2, pp. 305–317, 1960.

[12] M. J. Lighthill, "Large-amplitude elongated-body theory of fish locomotion," *Proceedings of the Royal Society of London B: Biological Sciences*, vol. 179, no. 1055, pp. 125–138, 1971.

[13] D. Barrett, M. Grosenbaugh, and M. Triantafyllou, "The optimal control of a flexible hull robotic undersea vehicle propelled by an oscillating foil," in *Proceedings of Symposium on Autonomous Underwater Vehicle Technology*, pp. 1–9, Monterey, CA, USA, 1996.

[14] J. Yu, M. Tan, S. Wang, and E. Chen, "Development of a biomimetic robotic fish and its control algorithm," *IEEE Transactions on Systems, Man and Cybernetics, Part B (Cybernetics)*, vol. 34, no. 4, pp. 1798–1810, 2004.

[15] S. D. Kelly, R. J. Mason, C. T. Anhalt, R. M. Murray, and J. W. Burdick, "Modelling and experimental investigation of carangiform locomotion for control," in *Proceedings of the 1998 American Control Conference. ACC (IEEE Cat. No.98CH36207)*, pp. 1271–1276, Philadelphia, PA, USA, 1998.

[16] J. Wang and X. Tan, "Averaging tail-actuated robotic fish dynamics through force and moment scaling," *IEEE Transactions on Robotics*, vol. 31, no. 4, pp. 906–917, 2015.

[17] C. Wang, G. Xie, L. Wang, and M. Cao, "CPG-based locomotion control of a robotic fish: using linear oscillators and reducing control parameters via PSO," *International Journal of Innovative Computing, Information and Control*, vol. 7, no. 7, pp. 4237–4249, 2011.

[18] W. Zhao, J. Yu, Y. Fang, and L. Wang, "Development of multimode biomimetic robotic fish based on central pattern generator," in *2006 IEEE/RSJ International Conference on Intelligent Robots and Systems*, pp. 3891–3896, Beijing, China, 2006.

[19] V. Kopman, J. Laut, F. Acquaviva, A. Rizzo, and M. Porfiri, "Dynamic modeling of a robotic fish propelled by a compliant tail," *IEEE Journal of Oceanic Engineering*, vol. 40, no. 1, pp. 209–221, 2015.

[20] K. A. Morgansen, B. I. Triplett, and D. J. Klein, "Geometric methods for modeling and control of free-swimming fin-actuated underwater vehicles," *IEEE Transactions on Robotics*, vol. 23, no. 6, pp. 1184–1199, 2007.

[21] G. Barbera, L. Pi, and X. Deng, "Attitude control for a pectoral fin actuated bio-inspired robotic fish," in *2011 IEEE International Conference on Robotics and Automation*, pp. 526–531, Shanghai, China, 2011.

[22] C. Yang, J. Luo, Y. Pan, Z. Liu, and C. Y. Su, "Personalized variable gain control with tremor attenuation for robot teleoperation," *IEEE Transactions on Systems, Man, and Cybernetics: Systems*, pp. 1–12, 2017.

[23] K. A. McIsaac and J. P. Ostrowski, "Motion planning for anguilliform locomotion," *IEEE Transactions on Robotics and Automation*, vol. 19, no. 4, pp. 637–652, 2003.

[24] Y. Li, R. Cui, Z. Li, and D. Xu, "Neural network approximation-based near-optimal motion planning with kinodynamic constraints using RRT," *IEEE Transactions on Industrial Electronics*, p. 1, 2018.

[25] Y. Xu, C. Yang, J. Zhong, N. Wang, and L. Zhao, "Robot teaching by teleoperation based on visual interaction and extreme learning machine," *Neurocomputing*, vol. 275, pp. 2093–2103, 2018.

[26] H. Asada and J.-J. Slotine, *Robot Analysis and Control*, John Wiley & Sons, 1986.

[27] M. W. Spong and M. Vidyasagar, *Robot dynamics and control*, John Wiley & Sons, 2008.

[28] C. Yang, Y. Jiang, W. He, J. Na, Z. Li, and B. Xu, "Adaptive parameter estimation and control design for robot manipulators with finite-time convergence," *IEEE Transactions on Industrial Electronics*, vol. 65, no. 10, pp. 8112–8123, 2018.

[29] D. R. Yoerger, J. G. Cooke, and J.-J. E. Slotine, "The influence of thruster dynamics on underwater vehicle behavior and their incorporation into control system design," *IEEE Journal of Oceanic Engineering*, vol. 15, no. 3, pp. 167–178, 1990.

[30] S. R. Buss, "Introduction to inverse kinematics with Jacobian transpose, pseudoinverse and damped least squares methods," *IEEE Journal of Robotics and Automation*, vol. 17, no. 1–19, p. 16, 2004.

[31] J.-J. E. Slotine W. Li et al., *Applied Nonlinear Control*, vol. 199, Prentice Hall, Englewood Cliffs, NJ, USA, 1991.

[32] M. Natrella, *NIST/SEMATECH e-Handbook of Statistical Methods*, National Institute of Standards and Technology, 2010.

[33] M. W. Spong, S. Hutchinson, and M. Vidyasagar, *Robot Dynamics and Control*, John Wiley Sons, Inc, Hoboken, NJ, USA, 1989.